



Original Research Article (Experimental)

In vivo anticancer effects of *Momordica charantia* seed fat on hepatocellular carcinoma in a rat model



K.N.K. Ranasinghe^a, A.D. Premarathna^a, T.A.N. Mahakapuge^a, K.K. Wijesundera^a,
A.T. Ambagaspitiya^a, A.P. Jayasooriya^b, S.A.M. Kularatne^c, R.P.V.J. Rajapakse^{a,*}

^a Department of Veterinary Pathobiology, Faculty of Veterinary Medicine and Animal Science, University of Peradeniya, Peradeniya, Sri Lanka

^b Department of Basic Veterinary Sciences, Faculty of Veterinary Medicine and Animal Science, University of Peradeniya, Peradeniya, Sri Lanka

^c Department of Medicine, Faculty of Medicine, University of Peradeniya, Peradeniya, Sri Lanka

ARTICLE INFO

Article history:

Received 25 December 2020

Received in revised form

26 February 2021

Accepted 1 March 2021

Available online 16 July 2021

Keywords:

Anticancer effect

In vivo

Momordica charantia

Hepatocellular carcinoma

Rat

ABSTRACT

Background: *Momordica charantia* or bitter melon is a well-known vegetable with a number of therapeutic actions in Ayurvedic medicine. Alpha-eleostearic acid, a conjugated trienoic fatty acid present in bitter melon is proven to have anticancer properties. Crude seed oil from local bitter melon varieties could be an effective and economical anticancer therapy.

Objective(s): The study was conducted to evaluate the anticancer effect of the crude oil from the seeds of Matala green variety of bitter melon on a hepatocellular carcinoma-induced rat model.

Materials and methods: Hepatocellular carcinoma (HCC) was experimentally induced in Wistar rats. Crude seed oil of Matala green bitter melon (MGBM) was supplemented to one treatment group in concurrence with carcinoma induction and to another treatment group after the development of carcinoma. After 168 days, gross morphological, histopathological, biochemical, hematological and gene-expression analysis of treated and control groups were performed.

Results: Oral supplementation of MGBM seed oil showed a statistically significant reduction ($p < 0.05$) in the average number, diameter and area of hepatic dysplastic nodules and a reduction in the size of histopathological neoplastic lesions in both treatment groups compared to the non-treated control group. The expression of tumor suppressor gene *p53* and anti-apoptotic gene *Bcl-2* were significantly increased while the expression of apoptotic gene *caspase 3* was significantly reduced in the treatment group when MGBM supplementation was in concurrence with carcinogenesis ($p < 0.05$).

Conclusion: Crude seed oil from the MGBM has anticancer effects against experimentally induced HCC in Wistar rats, specially when supplemented in concurrence with carcinoma induction.

© 2021 The Authors. Published by Elsevier B.V. on behalf of Institute of Transdisciplinary Health Sciences and Technology and World Ayurveda Foundation. This is an open access article under the CC BY-NC-ND license (<http://creativecommons.org/licenses/by-nc-nd/4.0/>).

1. Introduction

Globally, cancer is known as the second leading cause of deaths. In 2018, there were an estimated 18.1 million new cases and 9.6 million deaths due to cancer [1]. Hepatocellular carcinoma (HCC) is the fifth most frequent primary malignancy of the liver worldwide [2]. In Sri Lanka, HCC incidence is on the rise. Conditions like cirrhosis, hepatitis B and hepatitis C infections are closely associated with the majority of HCCs [3]. Mortality of HCC is found to be

increased mainly due to poor prognosis and lack of effective treatment options [4]. Conventional treatments for HCC include chemotherapy, radiation therapy and surgical resection [5]. Although effective current treatments are limited, chemotherapy provides much better hope for HCC patients, either alone or in combination with other therapies. Radiation therapy is also widely used to shrink tumor mass before surgical resection or to destroy any remaining cancer cells after the surgical resection [6].

Conventional cancer treatments are widely practiced throughout the world increasing survival rates of many patients successfully. However, some patients are experiencing incomplete remission and several side effects [7]. Furthermore, these treatments are expensive and not affordable by some people, especially in developing countries. Thus, it is of paramount importance to

* Corresponding author.

E-mail: jayanthar@pdn.ac.lk

Peer review under responsibility of Transdisciplinary University, Bangalore.

identify natural plant-based preventive medicines having potent anti-carcinogenic activity and cheap production cost [8].

Bitter melon (*Momordica charantia*; family Cucurbitaceae), also known as bitter gourd or *karawila*, is a herb found in several tropical and subtropical countries. It is a slender, climbing annual vine with long-stalked leaves and yellow male and female flowers. The bitter melon fruit is utilized as a vegetable and also offers several components which exhibit medicinal activities against a number of diseases in Ayurvedic medicine. Fruits, vine, leaves and roots of this plant have been used in traditional medicine as a remedy for diabetes, hypertension, arthritis, cardiovascular diseases, ageing and obesity, toothaches, diarrhea, malaria, viral and bacterial infections, pains, stomach disorders and all types of inflammations [9,10].

Many different varieties of bitter melon are grown worldwide [11]. Global climatic changes and soil nature usually alter the chemical composition of plants [12,13]. In Sri Lanka, several varieties of bitter melon (*Thinnaweli*, MC43, Matale green, *kalu karawila*, *geta karawila*, SM1) are available. The seeds are usually discarded in the process of cooking [14]. Crude bitter melon seed oil (BMO) has been tested for its anticancer effects in many studies. Crude BMO rich diets have reduced azoxymethane (AMO) induced colon cancer incidence in dose-dependant manner in rats [15]. Another study has proven the induction of differentiation of leukemia cell HL60 in a dose-dependent manner [16]. Further evaluation of BMO showed it contains conjugated trienoic fatty acids with 18 carbon atoms. They are in the form of conjugated linolenic acids and account for 56.2% of the total fatty acid profile of seed lipids. It is also named α -eleostearic acid (α -ESA, 9Z11Z13E-18:3) [17]. In previous studies, fatty-acid profile of BMO has been revealed by gas chromatography. α -ESA accounted for 59.1 mol % which is reported to have strong antitumor effects on human tumor cells and it is even more potent than the well-known anticancer fatty acid, conjugated linoleic acid (CLA) [18–20]. Most importantly, it has also been reported that α -ESA is rapidly and completely converted into CLA *in vivo* [21]. A strong anti-carcinogenic effect of α -ESA has been demonstrated *in vitro* using human tumor cell lines including DLD-1 (colon adenocarcinoma), Hep 2 (hepatoma), A549 (lung adenocarcinoma) and HL-60 (acute promyelocytic leukemia) and *in vivo* using DLD-1 cells transplanted into nude mice [22].

The effective, cheap and easy crude extraction of BMO from Sri Lankan *karawila* varieties will aid in developing local scientifically proven inexpensive anticancer drug(s) against HCC. The present study was designed to evaluate *in vivo* anticancer effects of crude BMO extracted from Matale green variety in chemically induced HCC. Tumor initiator, genotoxic diethylnitrosamine (DEN) and the tumor promoter, non-genotoxic thioacetamide (TAA) were used to induce HCC in rats as described by Omura et al., 2014 [23]. Anticancer effects of crude BMO was evaluated based on gross and histopathological changes in the liver and relative gene expression levels of selected genes including tumor suppressor *p53*, oncogene *BCL2* and apoptotic promoting factor *caspase 3*.

2. Materials and methods

2.1. Ethical statement

All experimental procedures were approved by Ethics Review Committee of the Faculty of Veterinary Medicine and Animal Science, University of Peradeniya, Sri Lanka.

2.2. Collection of plant material and authentication

Dried seeds of Matale green variety of *Momordica charantia* L. (English: bitter melon, bitter gourd; local: *Karawila*) were

purchased from the Department of Agriculture, Gannoruwa, Sri Lanka. Mature Matale green variety of *M. charantia* collected from the same place (Central province, Sri Lanka, 7°26'99"N, 80°59'38"E) was authenticated by the Royal Botanical Gardens, Peradeniya, Sri Lanka and the voucher specimen was deposited (voucher specimen no KNKMC1) at the same institute.

2.3. Extraction of seed oil

Husks of seeds of bitter melon were removed manually. Kernels were dried under mild heat (37°C) for 2 h and they were infused to Mini Oil Expeller (China) to gain pure seed oil (50% recovered). Obtained pure seed oil was stored at 4 °C until use.

2.4. Experimental animals and study design

Fifty, eight-weeks-old female Wistar rats (average body weight 235 g) were obtained from the Medical Research Institute (MRI), Sri Lanka. All rats were housed in an animal room and maintained at 22 ± 3°C with a 12-h light–dark cycle. All the animals were fed with a standard pellet diet (ingredients were wheat flour, rice flour, poultry starter feed, grounded maize, pedigree and milk powder) and provided with water *ad libitum*.

After acclimatizing rats for 7 days, they were divided into five equal experimental groups. HCC was induced in rats in groups 1, 2 and 3 (n = 10) (Fig. 1). Briefly, rats in these groups were injected with diethylnitrosamine (30 mg/kg BW, intraperitoneally) at day 0, followed by oral administration of thioacetamide (45 mg/kg BW at three days intervals) for 56 days [23]. HCC induction was confirmed by ultrasonography. Daily dosage of BMO for rats was calculated using a previously described formula [24]. Rats in group 1, group 2, group 3 and group 4 were treated with respective treatment of 100 µl of BMO (orally, daily) and TAA (45 mg/kg BW, orally, at three days intervals) by oral gavage as described in Fig. 1. Rats in the normal control group were given an equivalent amount of normal saline (orally, daily) from day 1 until day 168. All animals were euthanized under isoflurane anesthesia at day 169 and samples were collected. Livers were removed from all animals. Tissues were immediately fixed in 10% neutral buffered formalin (10% NBF). Formalin-fixed tissues were embedded in waxed and sectioned at 3–5 mm in thickness. Formalin-fixed, dewaxed sections were stained with hematoxylin and eosin (HE) for histopathology. Liver sections were imaged and gross measurements such as counts of dysplastic nodules in selected area (200 µm × 200 µm), diameter of dysplastic nodules (µm) and area of dysplastic nodules (µm²) were measured.

2.5. Haematology and serology

Heart blood (3 ml) was collected at the time of euthanasia by cardiac puncture and was used for haematological and serological analysis. White blood cell (WBC) count, red blood cell (RBC) count, packed cell volume (PCV) and total protein levels of all rats were determined. Serum glutamic-oxaloacetic transaminase (SGOT), serum glutamic-pyruvic transaminase (SGPT) and serum creatinine levels were determined using commercially available test kits according to the manufacturer's instructions (Human Gesellschaft für Biochemica und DiagnosticambH, Germany).

2.6. RNA extraction and reverse transcription - quantitative polymerase chain reaction (RT-qPCR)

Total RNA was extracted from frozen liver tissues using a RNA extraction kit (Bio & Sell RNA mini kit, Lohweg, Germany) according to the manufacturer's instructions. Quantification of RNA

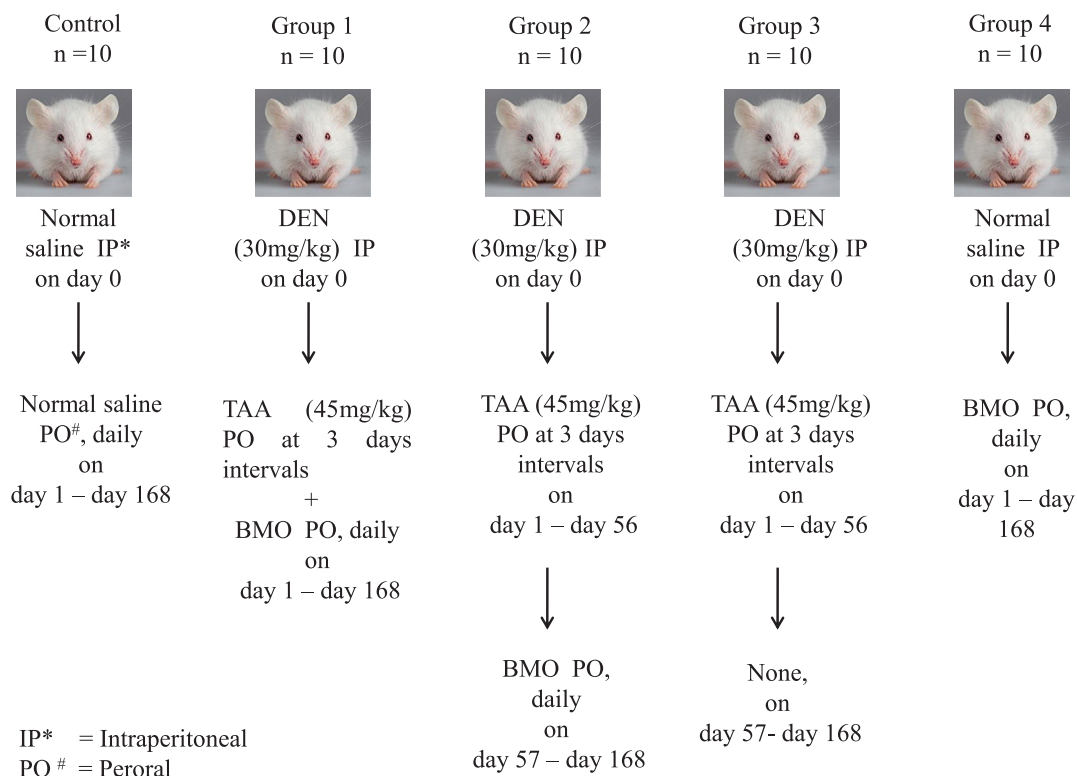


Fig. 1. Schematic representation of the experimental design in five experimental groups of rats (n = 10).

was performed using a NanoDrop spectrophotometer (NanoDrop 2000, Thermo Fisher, USA). Total RNA (100 ng) was reverse transcribed using a high-capacity cDNA reverse-transcription kit (Thermo Fisher Scientific, Waltham, USA). cDNA was stored at -20 °C until used. Gene-transcription analysis was performed using QuantStudio™ 6 and 7 Real-Time RT-PCR system (Applied Biosystem, USA). Primer pairs of selected genes were designed using Primer-Blast software (NCBI, Rockville Pike, USA) with 60 °C melting temperature (Tm). All primers were designed to span exon–exon junctions with GC% between 50% and 70%. The primers used are shown in Table 1. Real-Time RT-qPCR was performed using Power SYBR™ Green PCR Master mix (Thermo Fisher Scientific, Waltham, USA) according to the manufacturer's instructions. RT-qPCR conditions included initial denaturation at 95 °C for 5 min followed by 40 cycles of 95 °C for 45 s and at 60 °C for 30 s. For all candidate genes, melt curve analysis was also performed to confirm the presence of single PCR product at 95 °C, at 55 °C for 10 s and at 95 °C for 15 s. Mean cycle number (Cq) was obtained from each and every sample for the calculation of relative expression ratios using the ΔΔCq method [25]. It is based on the expression ratio of a target gene versus the

reference gene. GAPDH was used as the internal reference gene (Table 1).

2.7. Statistical analysis

Data were analyzed by using a one-way analysis of variance (ANOVA). GraphPad Prism, ver. 7.0 (GraphPad Software, CA, USA) was used for the analysis. A value of probability p < 0.05 was considered to indicate a statistically significant difference.

3. Results

Food and water intake of rats were normal throughout the study period. Mean body weight of rats (day 56) were 243.4 ± 7.2, 210.9 ± 53.8, 227.9 ± 86.9, 219.8 ± 48.1 and 269.8 ± 70.7 for normal control, group 1, group 2, group 3 and group 4 respectively. Moreover, on euthanized day, mean body weight of rats were 321.0 ± 76.9, 292.2 ± 95.3, 295.8 ± 114.8, 294.7 ± 63.3 and 348.6 ± 99.2 for normal control, group 1, group 2, group 3 and group 4 respectively. All rats in 5 experimental groups were survived until the end of the study.

Table 1
Primer sequences used in RT-qPCR.

Primer Name	Accession No	Size of Amplicon (bp) ^a	Annealing Temperature (°C)	Primer Sequences 5' to 3'
p53	NM_030989.3	187	60	F:CCCTGAAGACTGGATAACTGT R:AACCTGCAACATCCTGGGG
BCI2	NM_017059.2	178	60	F:AAGAAGCTGAGCGAGTGTCTC R:AGTAGAAAAGGGCAACCACCC
Caspase 3	NM_012922.2	169	60	F:GGAGCTTGAACGGAAGAA R:ACACAAGCCCATTTACAGGCT
GAPDH	NM_017008.4	74	60	F:GCAAGAGAGAGGCCCTCAG R:TGTGAGGAGATGCTCAGTG

^a Base pairs; F, Forward; R, Reverse.

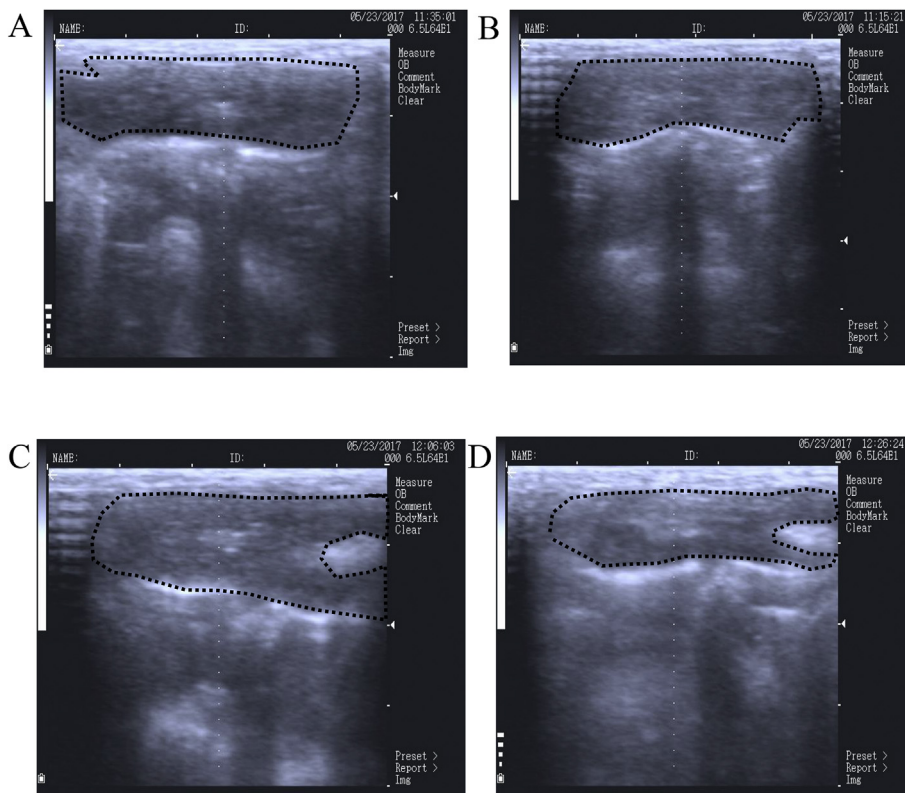


Fig. 2. Scanning images of liver (on the day 57). A (normal control, treated only normal saline): Normal sized clear liver; B (group 1- concurrent HCC induction and BMO treatment): Normal sized clear liver, no dysplastic nodules visible; C (group 2- HCC induction followed by BMO treatment/group 3- HCC induction with no treatment): High numbers of dysplastic nodules presence on the surface, hepatic enlargement is visible; D (group 4 - given BMO only): Normal sized clear liver.

3.1. Ultrasonography

HCC induction was confirmed by the scanning of the rat liver using ultrasonography at the end of DEN/TAA treatment.

Ultrasonographic images of livers in control group (Normal control), group 1 (concurrent HCC induction and BMO treatment) and group 4 (BMO only) were normal in appearance (Fig. 2A, B and D). Higher numbers of dysplastic nodules with

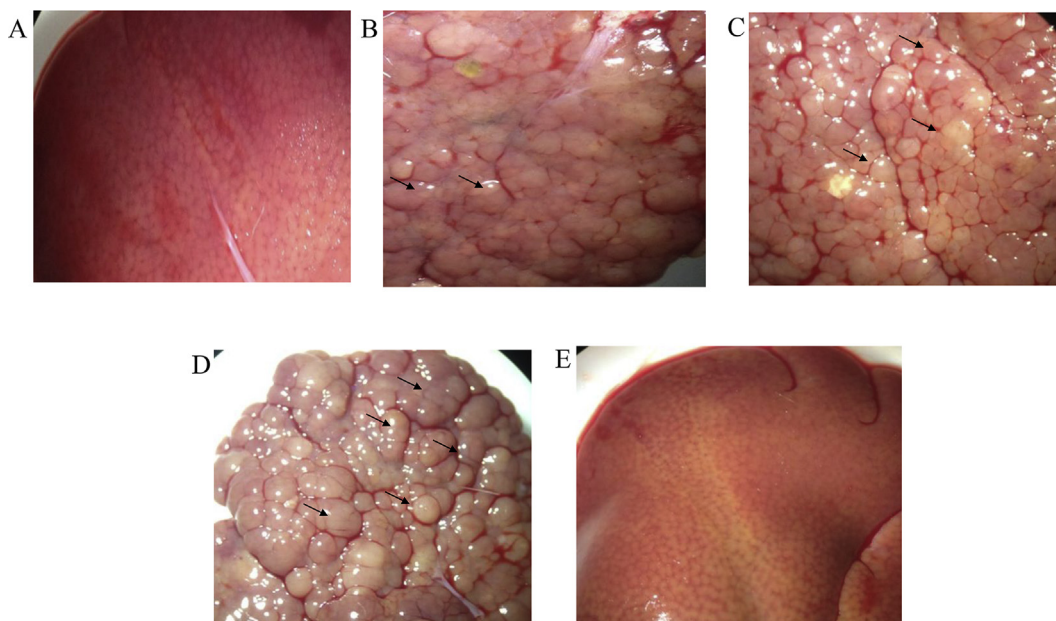


Fig. 3. Liver morphology observed under the light microscope ($\times 10$), Arrows indicate the presence of dysplastic nodules, A (normal control, treated only normal saline): Normal, healthy rats showing absence of nodules on the surface of liver; B (group 1-concurrent HCC induction and BMO treatment): A few nodules on the surface of the liver; C (group 2-HCC induction followed by BMO treatment): Some nodules on the surface of liver; D (group 3-HCC induction with no treatment): Many nodules on the surface of liver; E (group 4-given BMO only): Absence of nodules on the surface of liver.

Table 2
Gross pathological parameters of HCC induced rat livers^a.

	Normal Control	DEN/TAA + BMO	DEN/TAA ↓ BMO	DEN/TAA	BMO only	
Average number of dn	None	4.6 ± 1.9 ^a	8.4 ± 1.7 ^b	8.1 ± 2.1 ^c	None	ab **** ac ****
Average diameter (µm) of dn	None	55.5 ± 10.6 ^a	80.4 ± 17.0 ^b	130.3 ± 31.8 ^c	None	ac **** bc *
Average area (µm ²) of dn	None	1035.0 ± 356.1 ^a	1464.0 ± 355.4 ^b	3077.0 ± 1626.0 ^c	None	ac **** bc **

^a Mean ± Standard Deviation (SD); dn: dysplastic nodules; Control and group 4: none of dn.

irregular surfaces were observed in livers of groups 2 (HCC induction followed by BMO treatment) and group 3 (HCC induction only) (Fig. 2C).

3.2. Gross pathology

Liver morphology was assessed just after euthanasia. Livers of the control group and group 4 showed normal hepatic architecture with smooth surfaces and sharp edges (Fig. 3A and E). Livers of group 1 (Fig. 3B) showed a few dysplastic foci (<1 mm) and dysplastic nodules (>1 mm), in comparison to control livers. Livers of group 2 showed a moderate number of dysplastic foci and nodules (Fig. 3C), in comparison to control livers. The livers of group 3 showed a higher number of dysplastic foci and nodules (Fig. 3D), in comparison to control livers. Average number of dysplastic nodules, average diameter of dysplastic nodules and average area of dysplastic nodules in group 1, group 2 and group 3 are presented in Table 2.

3.3. Weights of liver

At p < 0.05 level, significantly increased liver weights were observed in group 3 compared with the normal control group (p = 0.0004) and a significantly increased liver index (liver weight/body weight) was observed in groups 2 and 3 when compared with the normal control group (p = 0.0003) (Table 3).

3.4. Histopathology

Normal liver architecture was observed in livers of normal control rats and those in group 4 (Fig. 4A and E). A few dysplastic nodules with nuclear atypia, hyperchromatism and vacuolar cytoplasm were observed in livers of group 1 and group 2 rats (Fig. 4B and C). An increased number of dysplastic nodules with prominent cellular nuclear atypia was observed in livers of group 3 (Fig. 4D).

3.5. Haematology

No parameters for the experimental groups differed significantly from those of the normal control group (Table 4). However, groups 1 and 2 had elevated WBC counts. Groups 1 and 2 also had lower total RBC counts, whereas RBC counts were higher in groups 3 and 4 relative to normal control (Table 4).

3.6. Serum chemistry

No parameters for the experimental groups differed significantly from those of the normal control group (Table 4). However, a declining tendency was observed in SGOT levels of groups 1, 2, 3 and 4 respectively.

3.7. Real-time quantitative RT-PCR

Relative gene expression of p53, a tumor suppressor gene, showed a statistically significant reduction in group 1 (Fig. 5A). However, no differences were evident in other groups in comparison with the normal control group. Anti-apoptotic BCL2 gene expression was significantly reduced in group 1, while group 2 showed reduced, but non-significant, level of gene. BCL2 gene expression levels in groups 3 and 4 were similar to those of the normal control group (Fig. 5B). Apoptosis promoting factor caspase 3 was scarcely expressed in the normal control group and in group 4 (fed BMO only). Groups 1, 2 and 3 showed increased expression, but this only reached statistical significance in group 1 (Fig. 5C).

4. Discussion

Initial intraperitoneal injection of DEN followed by oral treatment with TAA is a well-known method of inducing HCC in rats [23,26,27]. DEN followed by TAA in drinking water was successful in inducing liver fibrosis and poorly differentiated hepatocellular carcinoma [28,29]. In our study, rats given an initial intraperitoneal DEN (30 mg/kg) followed by oral TAA (45 mg/kg) once in every three days for two months developed HCC. It was proven by abdominal ultrasonography at day 57, gross and histopathology at the day of euthanasia.

Continuous daily treatment with BMO has proven to be a successful treatment for HCC, as evident in the current study. This finding is compatible with that of Ali et al., wherein treated methanol extract of *M. charantia* (MEMC) was used. HCC-induced albino rats by DEN along with oral supplementation of MEMC showed effective evidences against tumorigenesis of HCC. Presence of antioxidants in MEMC had reduced the oxidative stress caused by DEN, inhibiting inflammation, angiogenesis, tumor growth and promoting apoptosis [30]. The richest fatty acid in BMO is α-ESA, a conjugated trienoic acid/conjugated linolenic acid, which possesses potent anticancer effect [17–19]. Anticancer effect of α-ESA rich BMO has been demonstrated *in vitro* on cancer cells. It shows less cell viabilities as the apoptosis induced by α-ESA via lipid

Table 3
Mean liver weights and liver index of rats^a.

Group	Body weights (g)	Liver weights (g)	Liver Index ^b
Normal Control	293.7 ± 33.0	8.6 ± 0.6	2.9 ± 0.2
DEN/TAA + BMO	223.3 ± 19.4 ^c	11.1 ± 2.4	4.9 ± 0.7
DEN/TAA ↓ BMO	238.7 ± 15.0	15.6 ± 1.6	6.5 ± 0.3 ^c
Den/TAA	254.5 ± 3.7	16.1 ± 1.7 ^c	6.3 ± 0.7 ^c
BMO only	279.3 ± 11.7	8.4 ± 0.1	3.0 ± 0.1

^a Mean ± Standard Deviation (SD).

^b Liver Index = Liver weight/Body weight.

^c Statistically significant (p < 0.05).

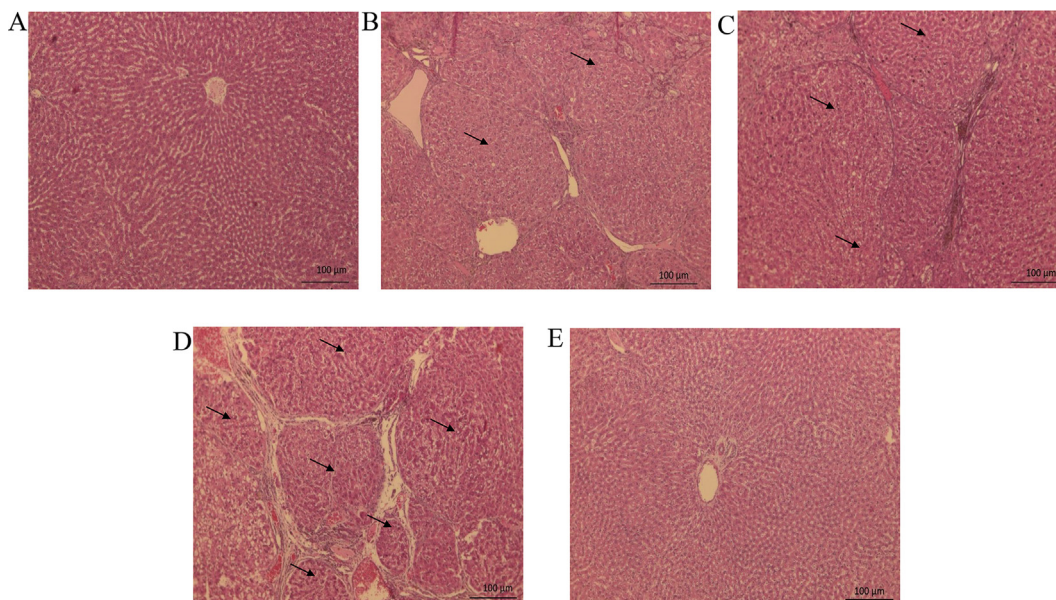


Fig. 4. Histopathological sections of liver tissues. Arrows indicate dysplastic nodules, A (normal control, treated only normal saline): Normal healthy rats showing normal architecture of liver cells and normal cell morphology; B (group 1-concurrent HCC induction and BMO treatment): Small neoplastic areas present; C (group 2-HCC induction followed by BMO treatment): Small neoplastic areas present; D (group 3-HCC induction with no treatment): Large, well demarcated neoplastic areas present. Liver cell damage is apparent in these rats; E (group 4-given BMO only): Normal architecture of liver cells indicate non-toxicity of BMO.

peroxidation as well as the activation of caspase-dependent pathway through the activation of *caspase 3*, *caspase 8* and *caspase 9* [22]. Another study suggested that suppression of VEGF-R-induced tumor angiogenesis is not only through lipid peroxidation, but through malnutrition via activation of the peroxisome proliferator-activated receptor (PPAR- γ) [20]. Furthermore, *in vivo* assays of BMO have demonstrated a significant reduction in the incidence of colonic adenoma and adenocarcinoma induced by a colonic carcinogen. There, α -ESA in BMO increases expression of PPAR- γ expression in the colonic mucosa [31]. Thus, anticancer effect of BMO could be due to the apoptosis via lipid peroxidation and caspase activation or angiogenesis suppression by activating PPAR- γ .

As demonstrated in the current study, the Matala green BMO effectively reduced HCC in the rat model. Previous research on anticancer effects of many plants have also shown the potential to reverse the DEN and TAA-induced carcinogenesis. With the treatment with Kynurenic acid, a tryptophan metabolite formed along kynurenine metabolic pathway in some food products, had limited liver cell damage reducing interstitial cellular infiltration and stagnation in the portal tract space limiting cellular necrosis in rat hepatocytes [32]. Curcumin, a biphenyl compound from

Curcuma longa L. rhizomes was reported to cause reversal of cellular damage caused by TAA in liver [33]. In another study, Silymarin, a polyphenolic flavonoid extracted from milk thistle, has been found to protect TAA-induced necrosis, apoptosis or mitosis in rat hepatocytes [34]. Administration of combination of grape seed extract which includes polyphenolic compounds and Silymarin effectively attenuate TAA induced hepatic fibrosis revealing its synergistic effect [35]. Moreover, phenolic compound-rich coriander leaf extract was shown to have reduced liver injury (few hepatic nodules and thinner fibrous septa) in TAA fed rat liver [36].

The possible influence of BMO treatment on selected genes related to tumor suppression was examined. The genes were *p53* (tumour suppressor gene), *Bcl2* (anti-apoptotic gene) and *caspase 3* (apoptosis promoting factor gene). Previously, *p53* has been referred to as the “guardian of the genome”. It conserves genome stability by preventing mutations [37–40]. However, in the current study *p53* gene expression was significantly reduced in group 1 where tumour mass development was least. Even though, a statistically significant difference was not observed, the highest *p53* expression was demonstrated by group 3, which had not been given BMO. Thus, we can assume that *p53*-mediated cellular

Table 4
Haematological and serological parameters of rats.

	Normal Control	DEN/TAA + BMO	DEN/TAA ↓ BMO	DEN/TAA	BMO only
WBC per mm ³ ($\times 10^4$)	2.3 \pm 0.8	2.6 \pm 0.4	2.6 \pm 0.3	2.2 \pm 0.2	2.3 \pm 0.2
RBC per mm ³ ($\times 10^6$)	6.7 \pm 0.3	6.2 \pm 1.1	6.1 \pm 0.9	7.7 \pm 1.1	7.6 \pm 0.7
PCV (%)	33.5 \pm 5.3	36.5 \pm 1.5	37.8 \pm 1.7	31.2 \pm 6.3	38.8 \pm 1.3
Total protein (g/dL)	7.1 \pm 0.8	8.0 \pm 0.7	7.5 \pm 0.5	6.3 \pm 1.1	7.6 \pm 0.3
SGOT/AST (IU/L)	223.9 \pm 58.3	209.8 \pm 14.2	206.6 \pm 25.9	202.5 \pm 26.9	170.3 \pm 30.1
SGPT/ALT (IU/L)	52.8 \pm 11.8	62.5 \pm 6.9	59.8 \pm 5.2	60.1 \pm 1.3	52.4 \pm 4.0
Creatinine(mg/dl)	0.8 \pm 0.1	0.6 \pm 0.3	0.8 \pm 0.0	0.9 \pm 0.1	0.8 \pm 0.1

Haematological and serological parameters of rats.
Data are presented as the Mean \pm SD of n = 10 rats of each experimental group.

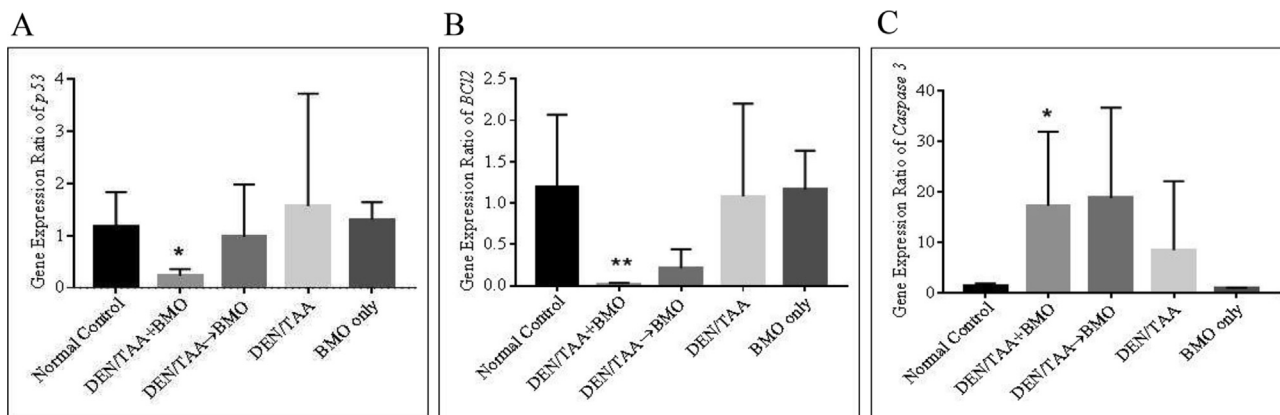


Fig. 5. Gene expression ratios of *p53*, *BCL2* and *caspase 3* genes. (Mean \pm SD). Internal control was *GAPDH*. A: Significant reduction of *p53* expression levels of group 1 (concurrent HCC induction and BMO treatment) rats compared with the normal control group (* $p < 0.05$). B: Significant reduction of expression levels of *BCL2* in group 1 rats compared with control group (** $p < 0.05$). C: Significantly increased expression of *caspase 3* levels in group 1 rats compared with the normal control group upon administration of BMO (* $p < 0.05$).

apoptosis is minimal in group 1 while it is highest in group 3. The increased *p53* gene expression in group 3 may be indicative of severe DNA damage and increased apoptosis of hepatocytes while BMO treatment significantly reduced these effects. Previously, increased levels of *p53* have been demonstrated in rat liver, with the induction of hepatic carcinomas using DEN, EMS, N–OH-AAF, N–OH-AABP [41].

BCL2 is an anti-apoptotic gene which inhibits the apoptosis of cancer cells, promoting their further growth [42]. We found a significant decrease in expression of *BCL2* when rats in group 1 were treated with BMO. Even though not statistically significant, group 2 also had lower *BCL2* expression indicating a higher rate of hepatocellular apoptosis. Previously, herbal treatment which included Nexrutine led to low expression levels of *BCL2*. It may result the increased expression levels of causing high ratio of *Bax/BCL2* which is most favourable for hepatic cell apoptosis [43]. Thus, both *p53* and *BCL2* genes showed reduced expressions in BMO-treated rats when compared with untreated rats.

We also found an increased expression of *caspase 3* with the BMO treatment in groups 1 and 2 compared with HCC-induced BMO non-treated rat liver in group 3. *Caspase 3* is an independent prognosis marker for HCC patients [44]. However, increased *caspase 3* expression in group 1 may be indicating good prognosis of HCC in rats treated with BMO. In BMO-untreated rats, *caspase 3* expression was lower agreeing with a poor prognosis of HCC. Furthermore, with the treatment of Nexrutine, increased *Bax/BCL2* ratio has been used as pro-apoptotic signal. Nexrutine caused release of cytochrome C proteins from mitochondria to cytoplasm. Apoptosome activation caused auto-activation and *caspase 3* activation [44]. In this study also, *caspase 3* activation was prominent after the BMO treatment. Hence, a possible effect of BMO treatment and the BMO-induced apoptosis is via the intrinsic pathway of apoptosis.

Even though reduction of HCC masses was observed grossly and histopathologically, no changes in serological profiles were evident between the rat groups. The results may be due to the severe damages caused to the liver for a longer period of time. The levels of serum enzymes did not show any significant differences between five experimental groups, making it difficult to explain the liver enzyme changes up on administration of DEN/TAA for rats.

5. Conclusion

The crude seed oil extracted from Matale green variety of bitter melon is an effective and inexpensive natural treatment against

cancer. The gross morphological, histopathological, biochemical, hematological and gene-expression data of the current study proved evidence for its anticancer effects. In the experimentally induced HCC rat model of this study, BMO treatment was most successful when it was administered in concurrence with HCC induction. However, the anticancer effect was evident even when BMO was administered after HCC induction. This concludes that BMO of Matale green bitter melon variety could be used not only as a treatment for HCC patients, but also could be an effective HCC preventive agent.

Source(s) of funding

Funds received by National Research Council (NRC), Sri Lanka, Grant No: NRC15-028.

Conflict of interest

None.

Acknowledgements

We would like to thank National Research Council (NRC), Sri Lanka under the grant (Grant No: NRC15-028), Dr. M. P. Paranagama, Department of Basic Sciences, Faculty of Denat Sciences, University of Peradeniya, Technical Officers, Mr. K.B.A.T. Bandara and Mr. N.A.N.D. Perera, Division of Parasitology, Department of Veterinary Pathobiology, Faculty of Veterinary Medicine and Animal Science, University of Peradeniya, Staff of Animal House, Faculty of Medicine, University of Peradeniya.

References

- [1] Latest Global Cancer Data. Cancer burden rises to 18.1 million new cases and 9.6 million cancer deaths in 2018. Geneva: World Health Organization; 2018. <https://www.who.int/cancer/PRGloboCanFinal.pdf?ua=1#:~:text=The/global/cancer/burden/is,women/die/from/the,disease>.
- [2] McEvoy SH, McCarthy CJ, Lavelle LP, Moran DE, Cantwell CP, Skehan SJ, et al. Hepatocellular carcinoma: illustrated guide to systematic radiologic diagnosis and staging according to guidelines of the American association for the study of liver diseases. *Radiographics* 2013;33:1653–68.
- [3] Herath HMMTB, Kulatunga A. Large hepatocellular carcinoma in a non-cirrhotic liver with peritoneal and omental metastasis in a healthy man: a case report. *J Med Case Rep* 2017;11:1–8.
- [4] Aleksic K, Lackner C, Geigl JB, Schwarz M, Auer M, Ulz P, et al. Evolution of genomic instability in diethylnitrosamine-induced hepatocarcinogenesis in mice. *Hepatology* 2011;53:895–904.

- [5] Baskar R, Lee KA, Yeo R, Yeoh KW. Cancer and radiation therapy: current advances and future directions. *Int J Med Sci* 2012;9:193–9.
- [6] Abbas Z, Rehman S. An overview of cancer treatments modalities. *IntechOpen* 2018:139–56.
- [7] Damyranov CA, Maslev IK, Pavlov S, Avramov L. Conventional treatment of cancer realities and problems. *Ann Complement Altern Med* 2018;1:1–10.
- [8] Balachandran P, Govindarajan R. Cancer - an ayurvedic perspective. *Pharmacol Res* 2005;51:19–30.
- [9] Gupta M, Sharma S, Gautam AK, Bhadauria R. *Momordica charantia* linn. (Karela): nature's silent healer. *Int J Pharmaceut Sci Rev Res* 2011;11:32–7.
- [10] Cho EJ, Sin SM, Choi JM, Lee S, Cho KM, Kim HY. Protective effects of the active fraction of bitter melon (*Momordica charantia*) on nitric oxide-induced oxidative stress in LLC-PK1 cell. *J Med Plants Res* 2012;6:4968–73.
- [11] Tan SP, Kha TC, Parks SE, Roach PD. Bitter melon (*Momordica charantia* L.) bioactive composition and health benefits: a review. *Food Rev Int* 2016;32:181–202.
- [12] Yeddes W, Wannas WA, Hammami M, Smida M, Chebbi A, Marzouk B, et al. Effect of environmental conditions on the chemical composition and antioxidant activity of essential oils from *Rosmarinus officinalis* L. Growing wild in Tunisia. *J Essent Oil-Bear Plants* 2018;21:972–86.
- [13] AbdElgawad H, Peshev D, Zinta G, Ende WVD, Janssens IA, Asard H. Climate extreme effect on the chemical composition of temperate grassland species under ambient and elevated CO₂: a comparison of fructan and non-fructan accumulators. *PLoS One* 2014;9:1–13.
- [14] Rathnayake AMGN, Abeyasinghe DC, Dharmadasa RM, Prathapasinghe GA, Jayasooriya LJAPA. Phytochemical, Physicochemical and mineral contents of domesticated and non domesticated populations of *Momordica charantia* L. Seeds harvested at two maturity stages. *World J Agric Res* 2018;6:77–81.
- [15] Kohno H, Yasui Y, Suzuki R, Hosokawa M, Miyashita K, Tanaka T. Dietary seed oil rich in conjugated linolenic acid from bitter melon inhibits Azoxymethane-induced rat colon carcinogenesis through elevation of colonic PPAR γ expression and alteration of lipid composition. *Int J Cancer* 2004;110:896–901.
- [16] Soundararajan R, Prabha P, Rai U, Dixit A. Antileukemic potential of *Momordica charantia* seed extracts on human Myeloid leukemic HL60 cells. *eCAM* 2012;2012:1–10.
- [17] Tanaka T, Hosokawa M, Yasui Y, Ishigamori R, Miyashita K. Cancer chemopreventive ability of conjugated linolenic acids. *Int J Mol Sci* 2011;12:7495–509.
- [18] Tsuzuki T, Tokuyama Y, Igarashi M, Nakagawa K, Ohsaki Y, Komai M, et al. α -Eleostearic acid (9Z11E13E-18:3) is quickly converted to conjugated linoleic acid (9Z11E-18:2) in rats. *J Nutr* 2004;134:2634–9.
- [19] Tsuzuki T, Kawakami Y, Abe R, Nakagawa K, Koba K, Imamura J, et al. Conjugated linolenic acid is slowly absorbed in rat intestine, but quickly converted to conjugated linoleic acid. *J Nutr* 2006;136:2153–9.
- [20] Tsuzuki T, Kawakami Y. Tumor angiogenesis suppression by α -eleostearic acid, a linolenic acid isomer with a conjugated triene system, via peroxisome proliferator-activated receptor γ . *Carcinogenesis* 2008;29:797–806.
- [21] Jayasooriya AP. How to safeguard an appropriate "all trans retinoic acid" concentration to keep cell division on track: exploring therapeutic hotspots from metabolomics. *Med Hypotheses* 2018;121:56.
- [22] Tsuzuki T, Tokuyama Y, Igarashi M, Miyazawa T. Tumor growth suppression by α -eleostearic acid, a linolenic acid isomer with a conjugated triene system, via lipid peroxidation. *Carcinogenesis* 2004;25:1417–25.
- [23] Omura K, Uehara T, Morikawa Y, Hayashi H, Mitsumori K, Minami K, et al. Detection of initiating potential of non-genotoxic carcinogens in a two-stage hepatocarcinogenesis study in rats. *J Toxicol Sci* 2014;39:785–94.
- [24] Guidance for industry. Estimating the maximum safe starting dose in initial clinical trials for therapeutics in adult healthy volunteers. USA: Food and Drug Administration; 2005. <https://www.fda.gov/media/72309/download>.
- [25] Livak KJ, Schmittgen TD. Analysis of relative gene expression data using real-time quantitative PCR and the $2^{-\Delta(\Delta Ct)}$ method. *Methods* 2001;25:402–8.
- [26] Heindryckx F, Colle I, Vlierberghe HV. Experimental mouse model for hepatocellular carcinoma research. *Int J Exp Pathol* 2009;90:367–86.
- [27] Newell P, Villanueva A, Friedman SL, Koike K, Llovet JM. Experimental models of hepatocellular carcinoma. *J Hepatol* 2008;48:858–79.
- [28] Park TJ, Kim HS, Byun KH, Jang JJ, Lee YS, Lim IK. Sequential changes in hepatocarcinogenesis induced by diethylnitrosamine plus thioacetamide in Fischer 344 rats: induction of gankyrin expression in liver fibrosis, pRB degradation in cirrhosis, and methylation of p16 (INK4A) exon 1 in hepatocellular carcinoma. *Mol Carcinog* 2001;30:138–50.
- [29] Henderson JM, Polak N, Chen J, Roediger B, Weninger W, Kench JG, et al. Multiple liver insults synergize to accelerate experimental hepatocellular carcinoma. *Sci Rep* 2018;8:1–12.
- [30] Ali MM, Borai IH, Ghanem HM, Abdel-Halim AH, Mousa FM. The prophylactic and therapeutic effect of *Momordica charantia* methanol extract through controlling different hallmarks of the hepatocarcinogenesis. *Biomed Pharmacother* 2018;98:491–8.
- [31] Moon HS, Guo DD, Lee HG, Choi YJ, Kang JS, Jo K, et al. Alpha-eleostearic acid suppresses proliferation of MCF-7 breast cancer cells via activation of PPAR γ and inhibition of ERK 1/2. *Cancer Sci* 2010;101:396–402.
- [32] Marciniak S, Wnorowski A, Smolinska K, Walczyna B, Turski W, Kocki T, et al. Kynurenic acid protects against thioacetamide-induced liver injury in rats. *Anal Cell Pathol* 2018;2018:1–11.
- [33] Abdou SE, Taha NM, Mandour AEA, Lebda MA, Hofi HRE, El-Morshedy. Anti fibrotic effect of Curcumin on thioacetamide induced liver fibrosis. *Alex J Vet Sci* 2015;45:43–50.
- [34] Kabiri N, Ahangar-Darabi M, Setorki M, Rafeian-kopaei M. The effect of silymarin on liver injury induced by thioacetamide in rats. *J HerbMed Pharmacol* 2013;2:29–33.
- [35] Nada SA, Gowifel AMH, El-Denshary EES, Salama AA, Khalil MG, Ahmed KA. Protective effect of grape seed extract and/or silymarin against thioacetamide induced hepatic fibrosis in rats. *J Liver* 2015;4:1–7.
- [36] Moustafa AHAM, Ali EMM, Moselhey SS, Tousson E, El-Said KS. Effect of coriander on thioacetamide-induced hepatotoxicity in rats. *Toxicol Ind Health* 2012;30:621–9.
- [37] Strachan T, Read AP. Human molecular genetics. 2nd ed. John Wiley & Sons Inc: USA and Canada; 1999.
- [38] Sionov RV, Haupt Y. The cellular response to p53: the decision between life and death. *Oncogene* 1999;18:6145–57.
- [39] Vousden KH, Lu X. Live or let die: the cell's response to p53. *Nat Rev Cancer* 2002;2:594–604.
- [40] Lacroix M, Toillon RA, Leclercq G. p53 and breast cancer, an update. *Endocr Relat Cancer* 2006;13:293–325.
- [41] Van Gijssel HE, Maassen CBM, Mulder GJ, Meerman JHN. p53 protein expression by hepatocarcinogens in the rat liver and its potential role in mitoinhibition of normal hepatocytes as a mechanism of hepatic tumour promotion. *Carcinogenesis* 1997;18:1027–33.
- [42] Hongfu L, Luping Z, Shaojie C, Zengxian W, Fei H, Dong W. The role and significance of bcl-2 and bax in the hepatic carcinoma. *Int J Morphol* 2012;30:1466–73.
- [43] Alam S, Yadav RS, Pal A, Purshottam SK, Chaudhari BP, Das M, et al. Dietary administration of nextrutine inhibits rat liver tumorigenesis and induces apoptotic cell death in human hepatocellular carcinoma cells. *Toxicol Rep* 2014;13:1–11.
- [44] Huang H, Zhang XF, Zhou HJ, Xue YH, Dong QZ, Ye QH. Expression and prognostic significance of osteopontin and caspase-3 in hepatocellular carcinoma patients after curative resection. *Cancer Sci* 2010;101:1314–9.